

Supporting Information

An Intuitive Hierarchical Assembly of Cluster–Organic Framework with 1.9 nm Thickness from Discrete Co₁₄ Cluster

Fu-Ping Huang,^{*a} Peng-Fei Yao,^a Hai-Ye Li,^a Qing Yu,^a He-Dong Bian,^{*b} and Hong Liang^a

Table of content:

1. Experimental Details

2. Structural Details

3. Measurement Details

1. Experimental Details

1.1. Synthesis of the compounds

Hydrothermal Synthesis of [Co₁₄(CH₃O)₄(dpbt)₆Cl₁₂]•14CH₃OH (1)

A mixture of 5,5'-di(pyridin-2-yl)-3,3'-bi(1,2,4-triazole) (H₂dpbt) (0.087 g, 0.3 mmol), CoCl₂·6H₂O (0.214 g, 0.9 mmol), and triethylamine (0.6 mmol, *ca.* 2 equiv per H₂dpbt) in MeOH/EtOH (v/v = 10:1, 11 mL) was sealed in a 25 mL Teflon-lined autoclave and heated at 130 °C in an oven for 3 days. Then it was allowed to be cooled to ambient temperature over 24 h, giving blue-green strip crystals of **1** in a yield of 31 % (base on H₂dpbt). Elemental analysis (%) calcd for Co₁₄C₁₀₂H₁₁₆N₄₈O₁₈Cl₁₂: C, 34.48; H, 3.29; N, 18.92; Found: C, 34.89; H, 3.08; N, 19.17. IR data for **1** (KBr, cm⁻¹): 3410(s), 1621(m), 1478(m), 1449(m), 1418(m), 1310(m), 1271(m), 1034(m), 803(m), 726(s).

The blue-green single crystals of **1** is not stable in air after breaking away from

liquid. We try to collecte the best single-crystal data for revealing the structural feature again and again. At last, under the temperature of 100 K, we get the best crystal data of **1** for the structural measurement up to now.

Hydrothermal Synthesis of [Co₁₄(CH₃O)₁₀(dpbt)₆Cl₆]•12CH₃OH (2)

Employing the same starting materials and same procedure, but higher concentrations of triethylamine (1.5 mmol, *ca.* 5 equiv per H₂dpbt), giving yellow hexagon crystals of **2** in a yield of 60 % (base on H₂dpbt). Elemental analysis (%) calcd for Co₁₄C₁₀₆H₁₂₆N₄₈O₂₂Cl₆: C, 36.77; H, 3.67; N, 19.42; Found: C, 36.47; H, 3.38; N, 19.76. IR data for **2** (KBr, cm⁻¹): 3423(s), 1620(m), 1477(m), 1448(m), 1418(m), 1311(m), 1270(m), 1033(m), 804(m), 727(s).

Discussion on the Synthesis of 1-2

The pH value of the initial reaction mixture may be modulated by varying the concentration of starting Et₃N, as a high pH values favor Et₃N in the equilibrium Et₃N + CH₃OH == Et₃NH⁺ + CH₃O⁻. To verify our conjecture, reaction mixtures with different starting concentration of Et₃N were prepared. Crystallization of **1** with an initial concentration of Et₃N (*ca.* 1.5-2.5 equiv per H₂dpbt) was always phase pure. Crystallization of **2** with an initial concentration of Et₃N (*ca.* 4-6.5 equiv per H₂dpbt) was always phase pure. However, when the initial concentration of Et₃N < 1.5 equiv, no crystals can be found; when concentration > 6.5 equiv, the Co(II) ions are almost precipitated; and when with the initial concentration (*ca.* 2.5-4 equiv), the complicated system of mixed crystals (**1** and **2**) have been obtained.

Synthesis of crystal(hexagon)-on-crystal(strip) phase 2/1

A mixture of as-synthesized **1** (*ca.* 20 mg of single crystals) and triethylamine (0.5 mmol) was added in 3 mL MeOH in a 20mL sealed vial at room temperature. After 72 h, there are flower-typed patterns gradually generated on the surface of the strip crystals of **1**. And then after 7 dates, hexagon crystals began to form. The growth of hexagon crystals on **1** allow to form the crystal(hexagon)-on-crystal(strip) phase . The shell crystal was carefully cut to collect Powder X-ray diffraction data. As time goes on, some attached hexagon crystals separate themselves from strip crystal of **1**.

The hexagon crystals were picked out and washed with MeOH solvent to collect single-crystal X-ray diffraction data (Table S3), and analyzed as $[\text{Co}_{14}(\text{CH}_3\text{O})_{10}(\text{dpbt})_6\text{Cl}_6] \cdot 12\text{CH}_3\text{OH}$ (**2**). Note the tightly sealed vial was heated in a preheated oven, can speed up the transformation process.

*Transformation from **1** to **2**.*

A mixture of as-synthesized **1** (ca. 40 mg of single crystals), triethylamine (1 mmol) and 3 mL MeOH were put together in a 10 mL vial. The tightly sealed vial was located in an oven at 100°C for 72 hours. The resulting yellow hexagon crystalline sample of **2** was collected and washed by MeOH with a yield of 46 % (base on **1**) (Figure S1).

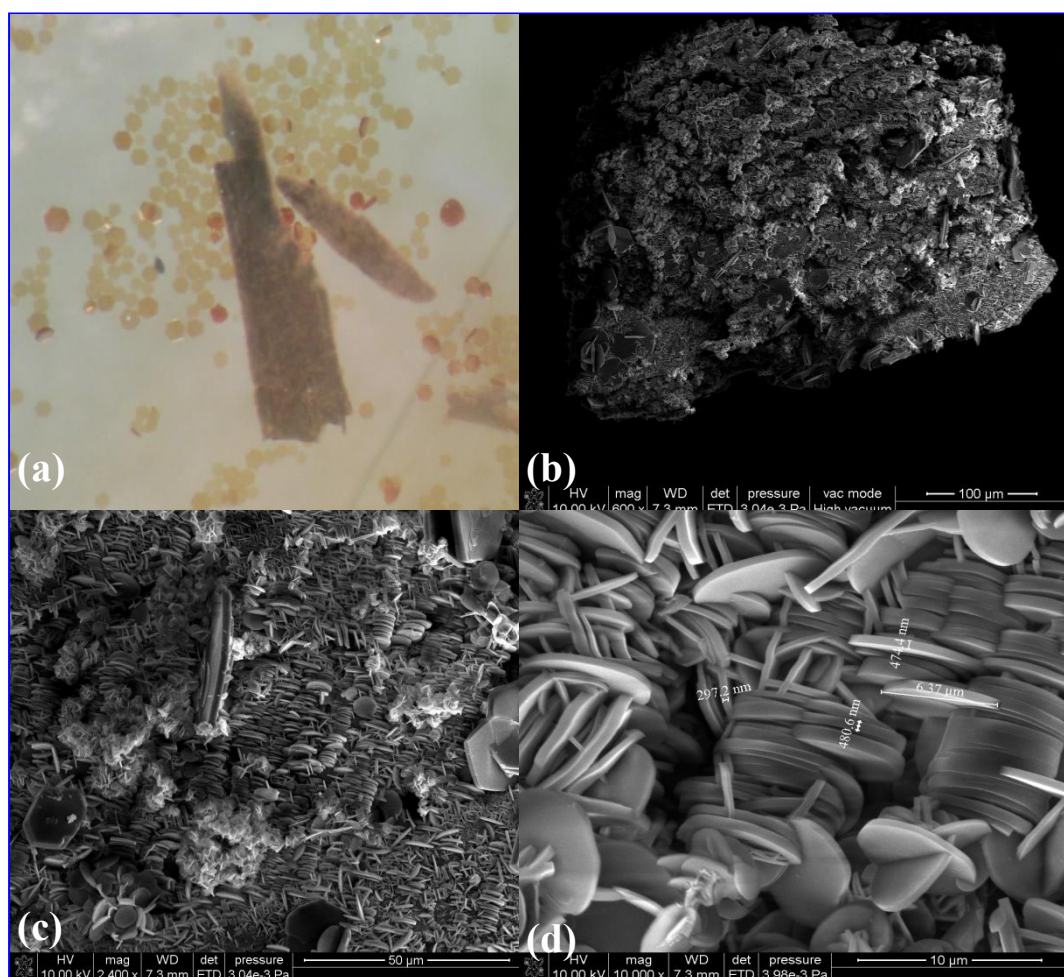


Figure S1 (a) Photographs of the product of the transformation, and the magnified SEM images of the strip crystals (100 μm for b, 50 μm for c, 10 μm for d) showing the growth of the hexagon crystals of **2** from **1**.

1.2. X-ray Crystallography

Single-crystal X-ray diffraction data collection for **1-2** were conducted on an Agilent Supernova diffractometer (Mo, $\lambda = 0.71073\text{\AA}$) at 100 and 298 K, respectively. The data were processed using CrysAlisPro. (Version 1.171.35.211). Preliminary orientation matrix and cell parameters were determined from three sets of scans at different starting angles. Data frames were obtained at scan intervals of 0.5° with an exposure time of 60 s per frame for **1**, and 30 s per frame for **2**, respectively. The structures were solved by direct methods and refined by full-matrix least-squares refinements based on F^2 within the SHELXTL Program package. Solvent molecules in **1-2** are significantly disordered and could not be modeled properly due to the lack of well defined atomic positions, thus the SQUEEZE procedure implemented in Platon (Spek, A. L. J. Appl. Crystallogr. 2003, 36, 7; Vander Sluis, P.; Spek, A. L. Acta Cryst. 1990. A46, 194) was used to calculate the solvent disorder area and remove its contribution to the overall intensity data. The Squeeze (or Bypass) procedure is a widely used and accepted method that corrects diffraction data for structures affected by the presence of heavily disordered solvent. However, the use of Squeeze does not impact the framework atoms. For **1**, SQUEEZE gives 505 electrons/unit cell for the voids. If these electrons are all from CH₃OH (18 e⁻), each unit cell has 28 (*ca.* 505/18) CH₃OH molecules, and each formula unit has 14 CH₃OH molecules (since Z = 2). So the suitable formula for this compound should be [Co₁₄(μ_3 -OCH₃)₄L₆Cl₁₂]·14CH₃OH. If other molecules (like EtOH or Et₃N) are mixed in the structure, it would become more complicated and not easy to assign them. For **2**, the contributions of some 431 electrons were removed from the formula unit. And as Z = 6 in this case, this could/might correspond with the removal of solvent such as 4 CH₃OH from the unit. Two Co(II) atoms (Co5 and Co6) are at a site with -3 symmetry and there are three Co(II)_{4.667} formula units in the unit cell. Therefore, the suitable formula for this compound may be {[Co₁₄(μ_3 -OCH₃)₄L₆(CH₃OH)₆Cl₆}·12 CH₃OH}_n. Additionally, the elemental analysis for **1-2** approve the result. The crystallographic details are summarized in Table S1. Selected bond distances and bond angles are

listed in Tables S2. Crystallographic data for the structural analyses have been deposited at the Cambridge Crystallographic Data Centre, reference numbers 1028478 for **1** and 1028479 for **2**, respectively.

1.3. Measurement Details.

The reagents and solvents employed were commercially available and used as received without further purification. The C, H, and N microanalyses were carried out with a Perkin–Elmer PE 2400 II CHN elemental analyzer. The FT-IR spectra were recorded from KBr pellets in the range 4000–400 cm⁻¹ on a Perkin–Elmer one FT-IR spectrophotometer. Raman spectra were obtained using a Renishaw in Via Raman microscope equipped with a 785 nm diode laser and a 1200 lines/mm grating. X-ray powder diffraction (XRPD) intensities were measured at 293 K on a Rigaku D/max-III A diffractometer (Cu-K α , $\lambda = 1.54056 \text{ \AA}$). The crystalline powder samples were prepared by crushing the single-crystals and scanned from 3–65° at a rate of 5°/min. Calculated patterns of **1–2** were generated with PowderCell. Mass measurements were conducted at a capillary temperature of 275 °C. Aliquots of the solution were injected into the device at 0.3mL/h. The ESI-MS and HPLC-MS mass spectrometry used for the measurements was a Bruker HCT and Thermo Exactive, respectively. and the data were collected in positive ion mode. All magnetic measurements (solid state) were carried out on a Quantum Design MPMS-XL SQUID magnetometer in a temperature range of 2.0–300 K and a DC field of 1000 Oe. Data were corrected for the diamagnetic contribution calculated from Pascal constants and the diamagnetism of the sample and sample holder were taken into account. The conversion from **1** to **2** have been tracked by Scanning Electron Microscope (SEM, FEI Quanta 200 FEG).

Table S1. Crystal data and structure refinement for **1–2 (squeezed)**:

Complex	1	2
Empirical formula	Co ₁₄ C ₈₈ H ₆₀ N ₄₈ O ₄ Cl ₁₂	(Co ₁₄ C ₉₄ H ₇₈ N ₄₈ O ₁₀ Cl ₆)/3
Formula weight	3104.24	1025.92

Crystal system	triclinic	trigonal
Space group	<i>P</i> -1	<i>P</i> -3
<i>a</i> (Å)	17.9278(4)	23.2046(4)
<i>b</i> (Å)	18.5740(4)	23.2046(4)
<i>c</i> (Å)	28.0345(6)	17.2439(19)
α (°)	74.8010(18)	90
β (°)	87.6211(18)	90
γ (°)	61.281(2)	120
Volume (Å ³)	7861.0(3)	8041.1(9)
<i>Z</i>	2	6
<i>D</i> _{calc} (g/cm ³)	1.286	1.271
Crystal size(mm ³)	0.44 × 0.10 × 0.08	0.40 × 0.30 × 0.24
θ range for data collection	2.78 to 25.02	2.93 to 25.24
Reflections collected	90048	35310
Independent reflections	27717, R(int) = 0.0322	9706, R(int) = 0.0317
Data/restraints/ parameters	27717/0/1509	9706/0/521
Goodness of fit (GOF)	1.144	1.090
Final <i>R</i> indices[<i>I</i> > 2σ(<i>I</i>)]	0.0941	0.0435
<i>R</i> indices (all data)	0.2773	0.0514

Table S2. Selected bond lengths (Å) and angles (°) for **1** and **2**.

1			
Co1—O1	2.079 (4)	Co7—Cl3	2.229 (7)
Co1—O2	2.156 (5)	Co7—N12	2.104 (7)
Co1—O3	2.098 (5)	Co7—N15	2.086 (8)
Co1—N3	2.180 (5)	Co8—N14	2.056 (7)
Co1—N22	2.256 (5)	Co8—N16	2.189 (8)
Co1—N27	2.181 (5)	Co8—N17	2.228 (7)
Co2—O1	2.129 (5)	Co8—N19	2.069 (6)
Co2—O2	2.130 (5)	Co8—N39	2.059 (6)
Co2—O4	2.105 (5)	Co8—N40	2.206 (7)
Co2—N30	2.188 (6)	Co9—Cl5	2.219 (3)

Co2—N35	2.187 (5)	Co9—Cl6	2.216 (3)
Co2—N43	2.210 (6)	Co9—N18	2.029 (6)
Co3—O2	2.153 (5)	Co9—N21	2.034 (6)
Co3—O3	2.100 (5)	Co10—N1	2.230 (6)
Co3—O4	2.124 (4)	Co10—N4	2.058 (5)
Co3—N7	2.233 (5)	Co10—N23	2.053 (6)
Co3—N11	2.192 (6)	Co10—N24	2.257 (6)
Co3—N47	2.185 (6)	Co10—N25	2.157 (6)
Co4—O1	2.095 (5)	Co10—N26	2.081 (5)
Co4—O3	2.129 (5)	Co11—Cl7	2.207 (4)
Co4—O4	2.111 (5)	Co11—Cl8	2.147 (4)
Co4—N13	2.183 (6)	Co11—N28	2.062 (6)
Co4—N20	2.209 (6)	Co11—N29	2.083 (7)
Co4—N38	2.216 (6)	Co12—N31	2.082 (6)
Co6—N6	2.076 (6)	Co12—N32	2.216 (7)
Co6—N8	2.266 (6)	Co12—N33	2.215 (6)
Co6—N9	2.184 (7)	Co12—N34	2.058 (6)
Co6—N10	2.071 (7)	Co12—N41	2.235 (7)
Co6—N46	2.087 (6)	Co12—N42	2.063 (6)
Co6—N48	2.249 (7)	Co13—Cl9	2.124 (5)
Co5—Cl1	2.208 (2)	Co13—Cl10	2.005 (6)
Co5—Cl2	2.1989 (18)	Co13—N36	2.029 (7)
Co5—N2	2.037 (5)	Co13—N37	2.048 (7)
Co5—N5	2.039 (6)	Co14—Cl11	2.269 (5)
Co7—Cl4	2.009 (16)	Co14—Cl12	2.120 (5)
Co7—Cl4'	2.171 (12)	Co14—N44	2.041 (6)
		Co14—N45	2.098 (6)
O1—Co1—O2	82.94 (18)	N46—Co6—N9	122.6 (3)
O1—Co1—O3	82.07 (18)	N46—Co6—N48	74.7 (2)
O1—Co1—N3	175.29 (19)	N48—Co6—N8	88.1 (2)
O1—Co1—N22	95.18 (19)	Cl4—Co7—Cl3	100.7 (5)
O1—Co1—N27	92.28 (18)	Cl4—Co7—Cl4'	71.1 (7)
O2—Co1—N3	92.75 (19)	Cl4—Co7—N12	107.7 (6)
O2—Co1—N22	173.7 (2)	Cl4—Co7—N15	154.3 (6)
O2—Co1—N27	95.62 (19)	Cl4'—Co7—Cl3	94.8 (5)
O3—Co1—O2	81.73 (18)	N12—Co7—Cl3	98.4 (3)
O3—Co1—N3	95.46 (19)	N12—Co7—Cl4'	166.8 (5)
O3—Co1—N22	92.08 (19)	N15—Co7—Cl3	103.4 (3)
O3—Co1—N27	173.99 (19)	N15—Co7—Cl4'	97.8 (5)
N3—Co1—N22	88.9 (2)	N15—Co7—N12	77.7 (3)
N3—Co1—N27	90.04 (19)	N14—Co8—N16	76.3 (3)
N27—Co1—N22	90.4 (2)	N14—Co8—N17	113.7 (3)
O1—Co2—O2	82.38 (18)	N14—Co8—N19	84.3 (3)
O1—Co2—N30	96.24 (19)	N14—Co8—N39	84.7 (3)

O1—Co2—N35	93.27 (19)	N14—Co8—N40	150.2 (3)
O1—Co2—N43	172.67 (19)	N16—Co8—N17	89.5 (3)
O2—Co2—N30	92.45 (19)	N16—Co8—N40	92.1 (3)
O2—Co2—N35	175.6 (2)	N19—Co8—N16	148.1 (3)
O2—Co2—N43	93.43 (19)	N19—Co8—N17	75.5 (2)
O4—Co2—O1	81.55 (18)	N19—Co8—N40	116.2 (3)
O4—Co2—O2	82.28 (18)	N39—Co8—N16	117.0 (3)
O4—Co2—N30	174.50 (19)	N39—Co8—N17	151.4 (3)
O4—Co2—N35	97.0 (2)	N39—Co8—N19	85.5 (2)
O4—Co2—N43	92.0 (2)	N39—Co8—N40	76.3 (2)
N30—Co2—N43	89.9 (2)	N40—Co8—N17	93.1 (2)
N35—Co2—N30	88.1 (2)	Cl6—Co9—Cl5	112.92 (11)
N35—Co2—N43	90.9 (2)	N18—Co9—Cl5	108.7 (2)
O2—Co3—N7	92.52 (19)	N18—Co9—Cl6	120.7 (2)
O2—Co3—N11	175.4 (2)	N18—Co9—N21	80.6 (3)
O2—Co3—N47	94.3 (2)	N21—Co9—Cl5	115.6 (2)
O3—Co3—O2	81.74 (19)	N21—Co9—Cl6	114.7 (2)
O3—Co3—O4	81.93 (18)	N1—Co10—N24	86.5 (2)
O3—Co3—N7	94.44 (19)	N4—Co10—N1	75.0 (2)
O3—Co3—N11	94.7 (2)	N4—Co10—N24	109.6 (2)
O3—Co3—N47	175.1 (2)	N4—Co10—N25	146.2 (2)
O4—Co3—O2	81.31 (18)	N4—Co10—N26	84.7 (2)
O4—Co3—N7	173.22 (19)	N23—Co10—N1	147.0 (2)
O4—Co3—N11	95.4 (2)	N23—Co10—N4	84.6 (2)
O4—Co3—N47	94.70 (19)	N23—Co10—N24	76.1 (2)
N11—Co3—N7	90.6 (2)	N23—Co10—N25	121.2 (2)
N47—Co3—N7	88.6 (2)	N23—Co10—N26	87.1 (2)
N47—Co3—N11	89.1 (2)	N25—Co10—N1	88.6 (2)
O1—Co4—O3	80.96 (18)	N25—Co10—N24	98.4 (2)
O1—Co4—O4	82.23 (18)	N26—Co10—N1	115.9 (2)
O1—Co4—N13	174.3 (2)	N26—Co10—N24	156.4 (2)
O1—Co4—N20	97.3 (2)	N26—Co10—N25	76.1 (2)
O1—Co4—N38	91.0 (2)	Cl8—Co11—Cl7	111.4 (3)
O3—Co4—N13	97.1 (2)	N28—Co11—Cl7	116.0 (2)
O3—Co4—N20	92.44 (19)	N28—Co11—Cl8	105.7 (2)
O3—Co4—N38	171.9 (2)	N28—Co11—N29	80.7 (2)
O4—Co4—O3	81.58 (18)	N29—Co11—Cl7	114.0 (2)
O4—Co4—N13	92.2 (2)	N29—Co11—Cl8	125.0 (2)
O4—Co4—N20	174.00 (19)	N31—Co12—N32	74.9 (2)
O4—Co4—N38	97.0 (2)	N31—Co12—N33	116.1 (2)
N13—Co4—N20	88.1 (2)	N31—Co12—N41	148.3 (2)
N13—Co4—N38	90.9 (2)	N32—Co12—N41	92.6 (3)
N20—Co4—N38	88.9 (2)	N33—Co12—N32	88.6 (2)
Cl2—Co5—Cl1	112.12 (9)	N33—Co12—N41	92.1 (2)

N2—Co5—Cl1	102.90 (16)	N34—Co12—N31	85.3 (2)
N2—Co5—Cl2	125.72 (16)	N34—Co12—N32	146.4 (3)
N2—Co5—N5	80.1 (2)	N34—Co12—N33	75.9 (2)
N5—Co5—Cl1	112.82 (18)	N34—Co12—N41	117.2 (3)
N5—Co5—Cl2	119.06 (16)	N34—Co12—N42	85.5 (2)
N6—Co6—N8	74.6 (2)	N42—Co12—N31	85.2 (2)
N6—Co6—N9	145.8 (3)	N42—Co12—N32	118.8 (2)
N6—Co6—N46	84.3 (2)	N42—Co12—N33	149.8 (3)
N6—Co6—N48	118.7 (2)	N42—Co12—N41	75.3 (2)
N9—Co6—N8	90.5 (3)	Cl10—Co13—Cl9	114.2 (4)
N9—Co6—N48	90.7 (3)	Cl10—Co13—N36	114.7 (4)
N10—Co6—N6	85.2 (2)	Cl10—Co13—N37	113.9 (4)
N10—Co6—N8	122.5 (3)	N36—Co13—Cl9	114.4 (3)
N10—Co6—N9	77.0 (3)	N36—Co13—N37	80.2 (3)
N10—Co6—N46	85.8 (2)	N37—Co13—Cl9	115.1 (3)
N10—Co6—N48	146.6 (3)	N44—Co14—Cl12	110.4 (3)
N46—Co6—N8	142.0 (2)	N44—Co14—N45	79.9 (2)
Cl12—Co14—Cl11	119.3 (3)	N45—Co14—Cl11	115.7 (2)
N44—Co14—Cl11	111.8 (3)	N45—Co14—Cl12	113.1 (2)

2 (Symmetry codes: (A) $-x+1, -y+1, -z+1$; (B) $-x+y, -x+1, z$; (C) $-y+1, x-y+1, z$.)

Co1—Cl1	2.3507 (17)	Co4—N2C	2.069 (3)
Co1—O1	1.957 (3)	Co4—N7	2.078 (3)
Co1—O2	2.025 (4)	Co4—N8	2.223 (4)
Co1—N12A	2.122 (4)	Co4—N9	2.249 (4)
Co1—N15A	2.088 (3)	Co4—N10	2.052 (4)
Co2—Cl2	2.3173 (14)	Co5—O4C	2.097 (3)
Co2—O1	1.996 (3)	Co5—O4	2.097 (3)
Co2—O2	1.998 (4)	Co5—O4B	2.097 (3)
Co2—N4	2.106 (3)	Co5—N13C	2.211 (3)
Co2—N5	2.185 (3)	Co5—N13B	2.211 (3)
Co3—O3	2.099 (2)	Co5—N13	2.211 (3)
Co3—O4	2.092 (2)	Co6—N14C	2.059 (3)
Co3—O4B	2.123 (2)	Co6—N14B	2.059 (3)
Co3—N3C	2.217 (3)	Co6—N14	2.059 (3)
Co3—N6	2.171 (3)	Co6—N16C	2.211 (3)
Co3—N11	2.205 (3)	Co6—N16B	2.211 (3)
Co4—N1C	2.210 (4)	Co6—N16	2.211 (3)
O1—Co1—Cl1	93.79 (12)	N2C—Co4—N9	148.67 (14)
O1—Co1—O2	76.76 (14)	N7—Co4—N1C	146.37 (14)
O1—Co1—N12A	162.14 (14)	N7—Co4—N8	75.18 (13)
O1—Co1—N15A	120.45 (14)	N7—Co4—N9	117.47 (15)
O2—Co1—Cl1	149.81 (13)	N8—Co4—N9	89.53 (14)
O2—Co1—N12A	93.60 (15)	N10—Co4—N1C	119.14 (15)
O2—Co1—N15A	101.73 (15)	N10—Co4—N2C	85.56 (13)

N12A—Co1—Cl1	87.09 (12)	N10—Co4—N7	85.49 (14)
N15A—Co1—Cl1	107.66 (11)	N10—Co4—N8	146.61 (15)
N15A—Co1—N12A	75.92 (13)	N10—Co4—N9	75.41 (13)
O1—Co2—Cl2	92.96 (11)	O4C—Co5—O4	81.46 (10)
O1—Co2—O2	76.50 (15)	O4C—Co5—O4B	81.46 (10)
O1—Co2—N4	113.44 (14)	O4—Co5—O4B	81.46 (10)
O1—Co2—N5	164.46 (14)	O4—Co5—N13C	92.98 (10)
O2—Co2—Cl2	145.18 (13)	O4C—Co5—N13C	95.54 (10)
O2—Co2—N4	100.80 (15)	O4B—Co5—N13C	174.00 (11)
O2—Co2—N5	90.38 (14)	O4C—Co5—N13B	92.98 (10)
N4—Co2—Cl2	113.75 (10)	O4—Co5—N13B	174.00 (11)
N4—Co2—N5	76.83 (12)	O4C—Co5—N13	174.00 (11)
N5—Co2—Cl2	93.21 (10)	O4B—Co5—N13B	95.54 (10)
O3—Co3—O4B	81.04 (10)	O4B—Co5—N13	92.98 (10)
O3—Co3—N3C	95.28 (11)	O4—Co5—N13	95.54 (10)
O3—Co3—N6	93.54 (11)	N13C—Co5—N13B	89.79 (11)
O3—Co3—N11	174.12 (13)	N13C—Co5—N13	89.79 (11)
O4—Co3—O3	81.75 (10)	N13B—Co5—N13	89.79 (11)
O4—Co3—O4B	80.96 (13)	N14C—Co6—N14B	85.86 (13)
O4—Co3—N3C	92.73 (11)	N14C—Co6—N14	85.86 (13)
O4B—Co3—N3C	173.07 (10)	N14B—Co6—N14	85.86 (13)
O4—Co3—N6	174.89 (11)	N14B—Co6—N16C	149.47 (13)
O4B—Co3—N6	96.41 (11)	N14C—Co6—N16C	75.64 (12)
O4B—Co3—N11	93.57 (10)	N14—Co6—N16C	116.17 (13)
O4—Co3—N11	95.16 (11)	N14C—Co6—N16B	116.17 (13)
N6—Co3—N3C	89.65 (12)	N14B—Co6—N16B	75.64 (12)
N6—Co3—N11	89.37 (12)	N14C—Co6—N16	149.47 (13)
N11—Co3—N3C	89.85 (12)	N14—Co6—N16B	149.47 (13)
N1C—Co4—N8	90.56 (14)	N14—Co6—N16	75.64 (12)
N1C—Co4—N9	92.19 (14)	N14B—Co6—N16	116.17 (13)
N2C—Co4—N1C	75.45 (13)	N16C—Co6—N16B	90.82 (13)
N2C—Co4—N7	84.87 (13)	N16C—Co6—N16	90.82 (13)
N2C—Co4—N8	118.74 (14)	N16B—Co6—N16	90.82 (13)
Co1—O1—Co2	104.30 (16)	Co2—O2—Co1	101.73 (17)
Co3C—O3—Co3B	98.22 (13)	Co3B—O3—Co3	98.22 (13)
Co3C—O3—Co3	98.22 (13)	Co3—O4—Co3C	97.67 (10)
Co3—O4—Co5	98.68 (10)	Co5—O4—Co3C	97.72 (10)

2. Structural Details

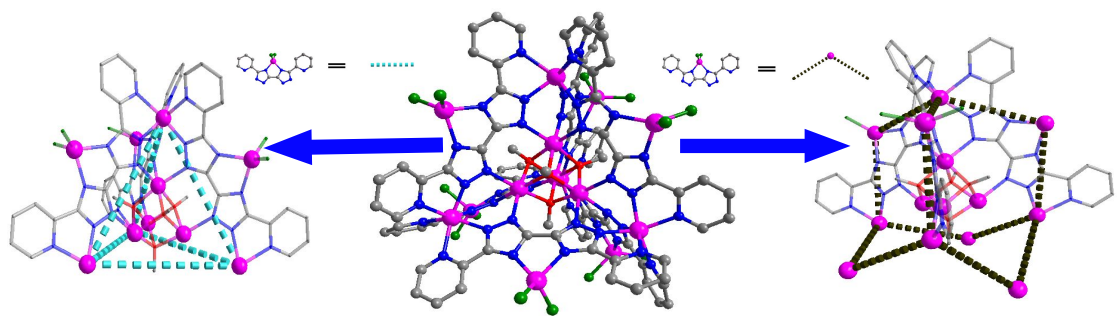


Figure S2 Ball and stick plot of $[\text{Co}_{14}(\text{CH}_3\text{O})_4(\text{dpbt})_6\text{Cl}_{12}]$ in **1** and the $\{\text{Co}_{14}\}$ unit corresponds to a distorted Co_{10} adamantane periphery encapsulate Co_4 cubic core.

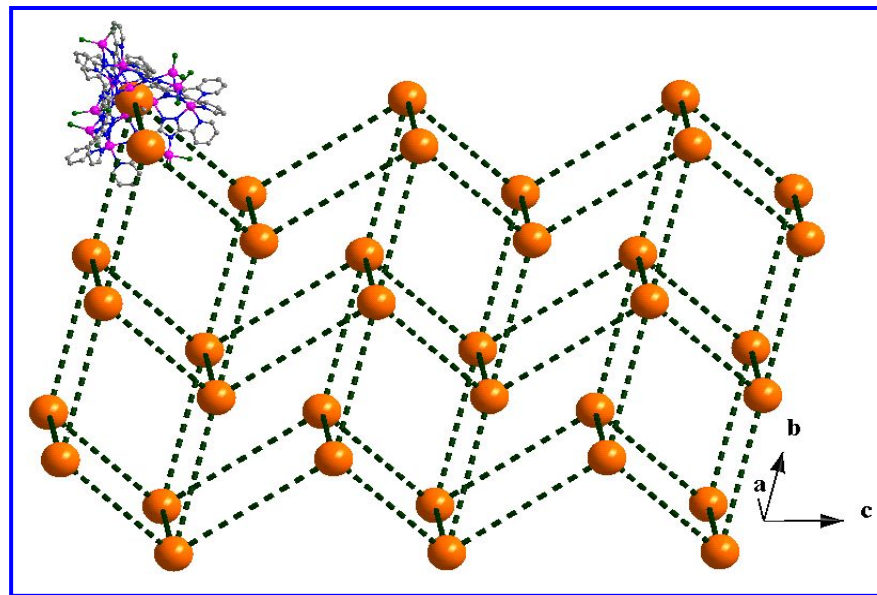


Figure S3 A packing-diagram of the supra-molecular balls (orange spheres) of **1** in the lattice.

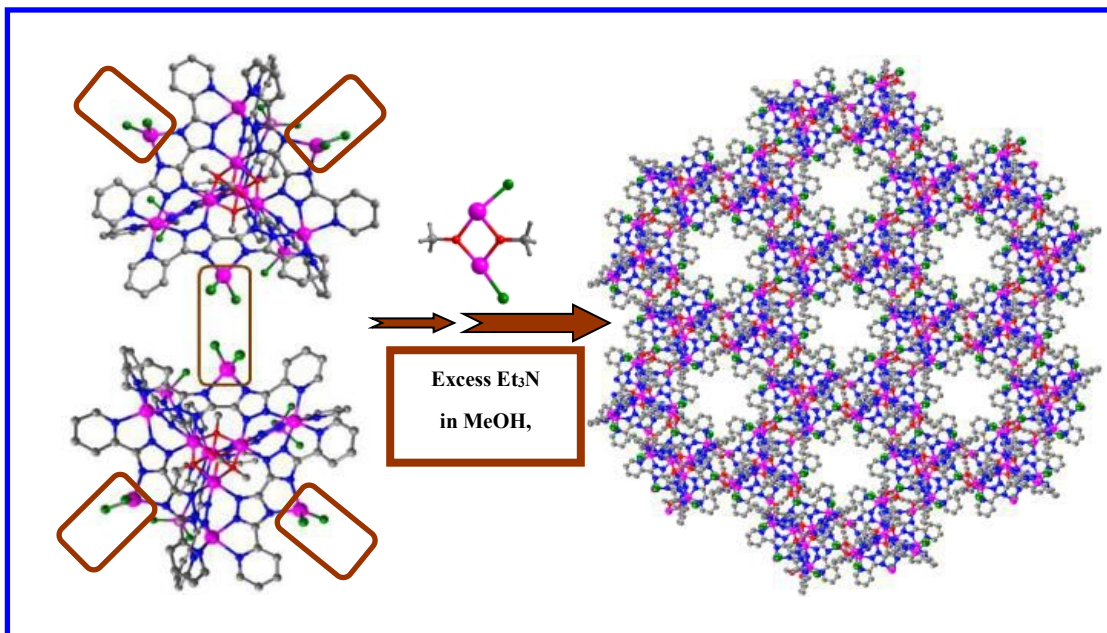


Figure S4 Crystal structures of **1** (left) and **2** (right). The coordination mode of CH_3O^- species linking neighboring clusters.

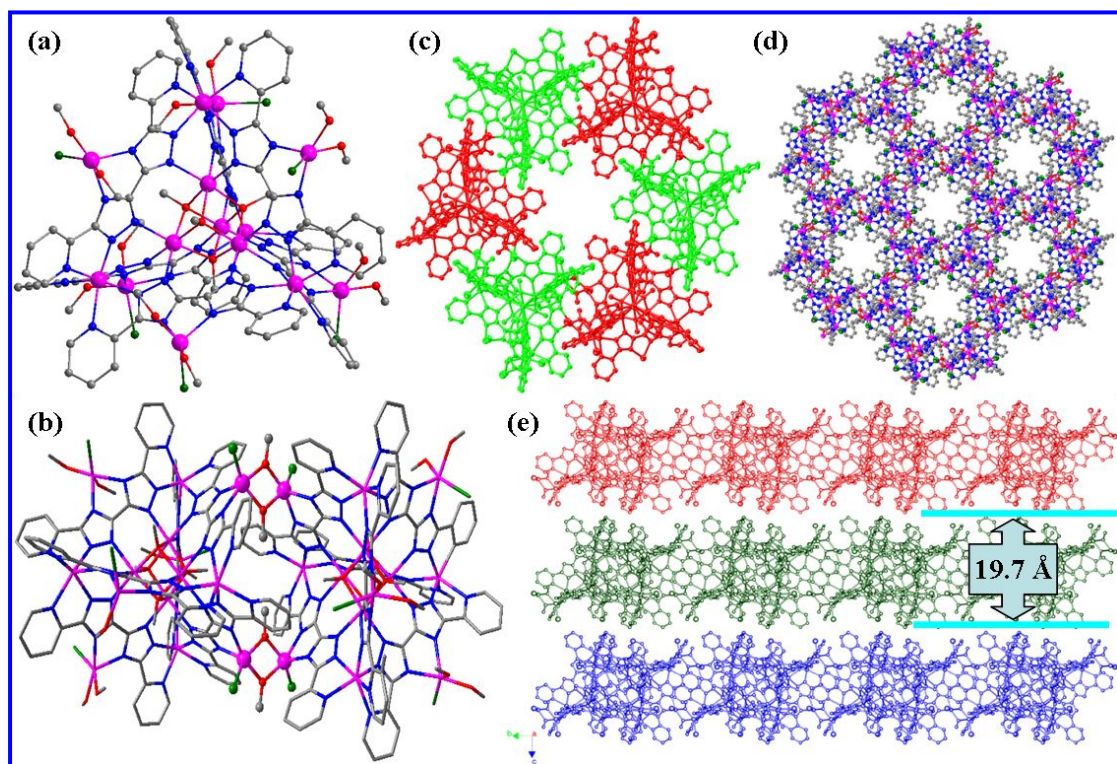


Figure S5 Structural characterization of **2**: (a) the local coordination environments of the Co(II) atoms; (b) The coordination mode of CH_3O^- groups linking neighboring clusters; (c-d) the 2-D honeycomb-type nanosheet; (e) the stacked supramolecular structure with the nanosheets.

3. Measurement Details

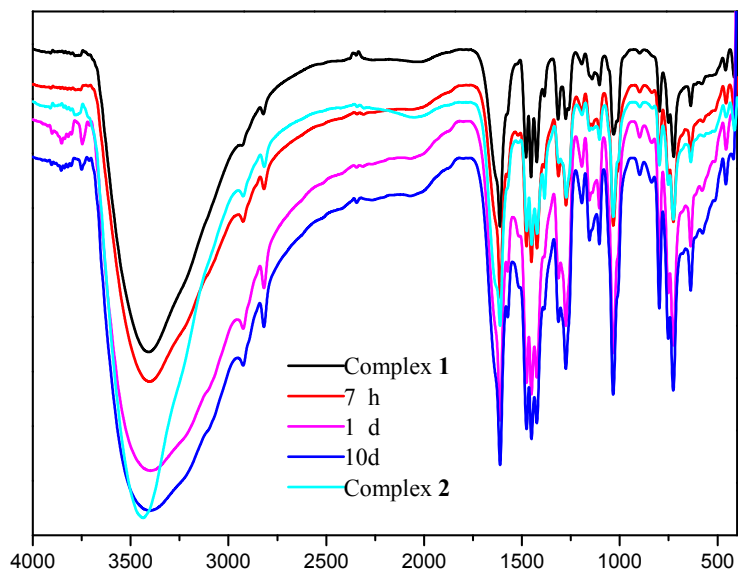


Figure S6 IR spectroscopy of **1** and **2**, and the Time-dependent IR spectroscopy for the conversion from **1** to **2**.

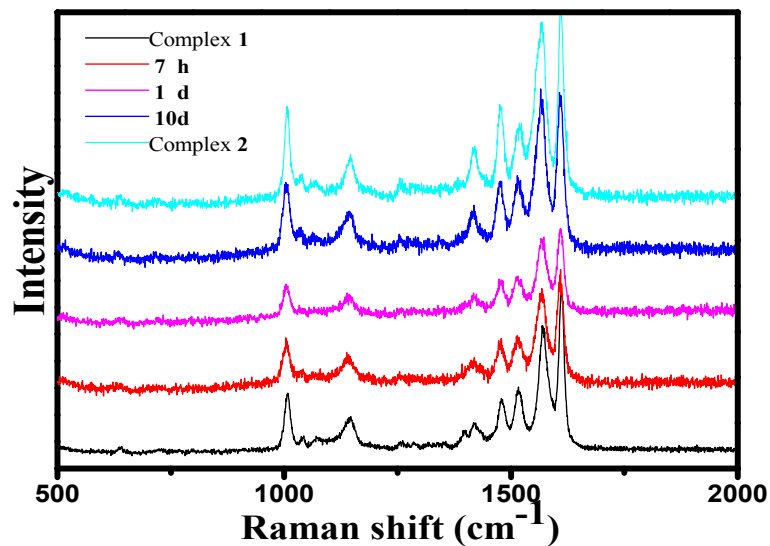


Figure S7 Raman spectroscopy of **1** and **2**, and the Time-dependent Raman spectroscopy for the conversion from **1** to **2**.

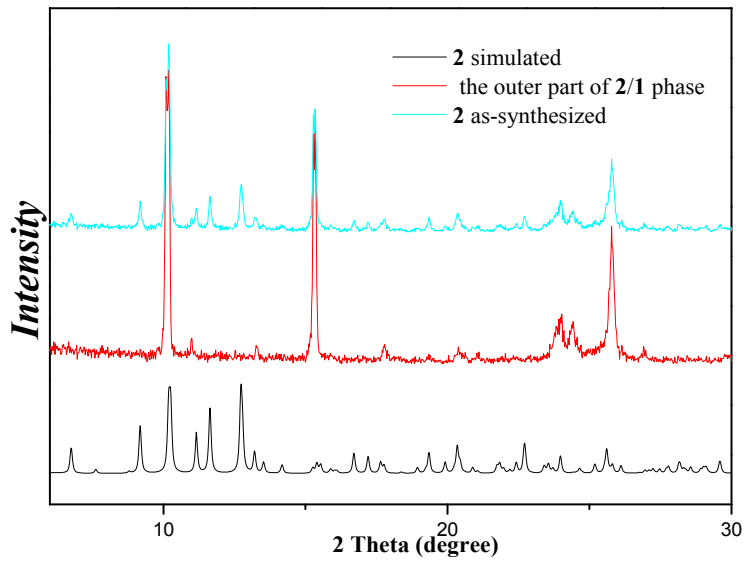


Figure S8. XRPD patterns of (black) simulated, (blue) as-synthesized **2**, (red) the outer part of **2/1** phase.

Table S3. The summary of the data collection, cell and refinement parameters from the single crystal X-ray diffraction.

Compounds	2 (as-synthesized)	2' (Transformation) (room temperature)	2'' (Transformation) (100 °C)
<i>a</i> (Å)	23.2046(4)	23.042(2)	23.138 (2)
<i>b</i> (Å)	23.2046(4)	23.042(2)	23.138 (2)
<i>c</i> (Å)	17.2439(19)	17.1957(13)	17.2201 (8)
α (deg)	90	90	90
β (deg)	90	90	90
γ (deg)	120	120	120
<i>V</i> (Å ³)	8041.1(9)	7906.6(12)	7983.9 (7)
Reflections collected	35310	18692	24010
Independent reflections	9706, R(int) = 0.0317	10591 R(int) = 0.1332	10849 R(int) = 0.1127
Data/restraints/parameters	9706/0/521	10591/0/521	10849/0/521
Final <i>R</i> indices[<i>I</i> > 2σ(<i>I</i>)] (squeezed)	0.0435	0.0840	0.0774
<i>R</i> indices (all data) (squeezed)	0.0514	0.222	0.1778

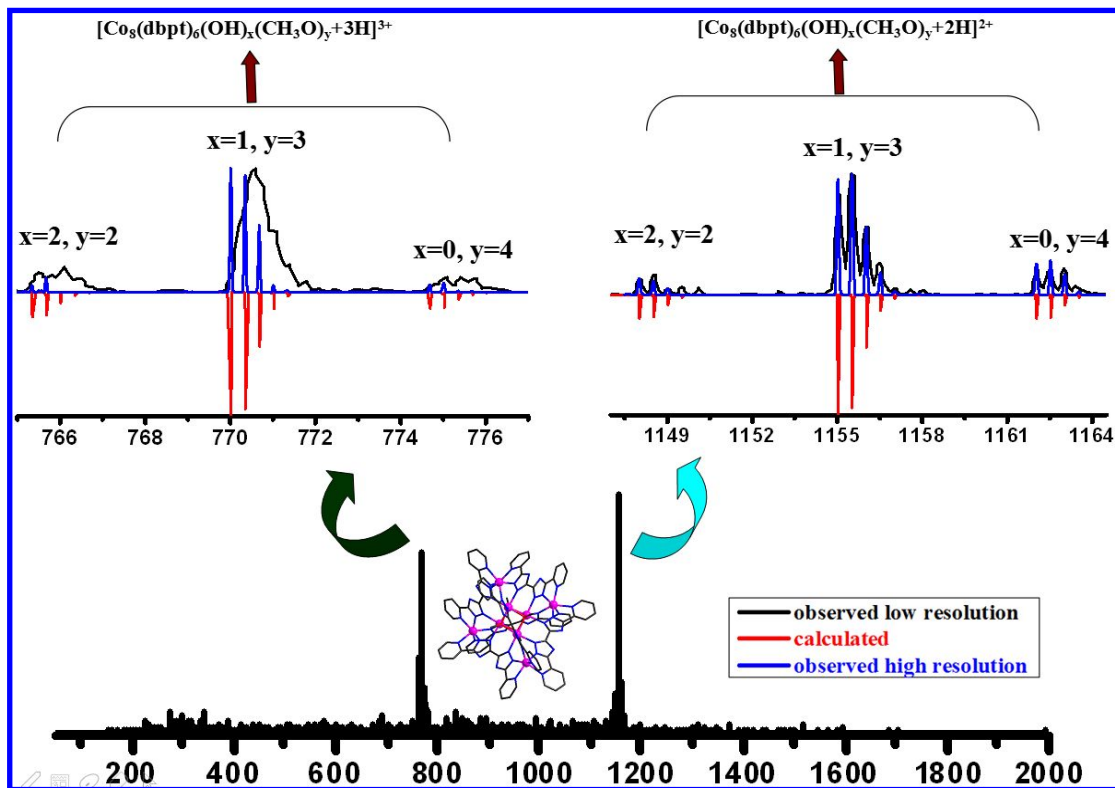


Figure S9. High/Low-resolution ESI-MS: overlay of the calculated (red) and observed (blue/black) peaks for the $[Co_8((OH)_x(CH_3O)_y(dpbt)_6 + 3H]^{3+}$ and $[Co_8((OH)_x(CH_3O)_y(dpbt)_6 + 2H]^{2+}$ ($x = 0-2$, $y = 2-4$) species.

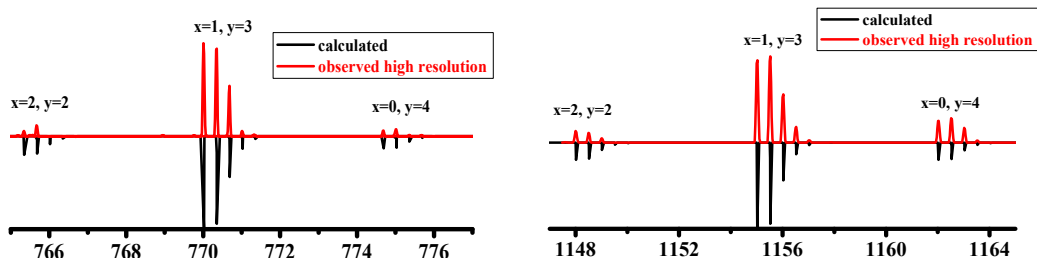


Figure S10. The expanded spectra of $[Co_8((OH)_x(CH_3O)_y(dpbt)_6 + 3H]^{3+}$ and $[Co_8((OH)_x(CH_3O)_y(dpbt)_6 + 2H]^{2+}$. Red: observed isotope patterns; Black: simulated isotope patterns.

Table S4. Peak assignments of the ESI-MS spectrum of **2**
 (the in-source energy was 50 eV) :

Typical Composition	Value of x, y	Observed	Calculated
	x=2, y=2	765.34	765.34
[Co ₈ (C ₁₄ H ₈ N ₈) ₆ (OH) _x (CH ₃ O) _y +3H] ³⁺	x=1, y=3	770.01	770.02
	x=0, y=4	774.69	774.69
	x=2, y=2	1148.00	1148.02
[Co ₈ (C ₁₄ H ₈ N ₈) ₆ (OH) _x (CH ₃ O) _y +2H] ²⁺	x=1, y=3	1155.03	1155.02
	x=0, y=4	1162.04	1162.03

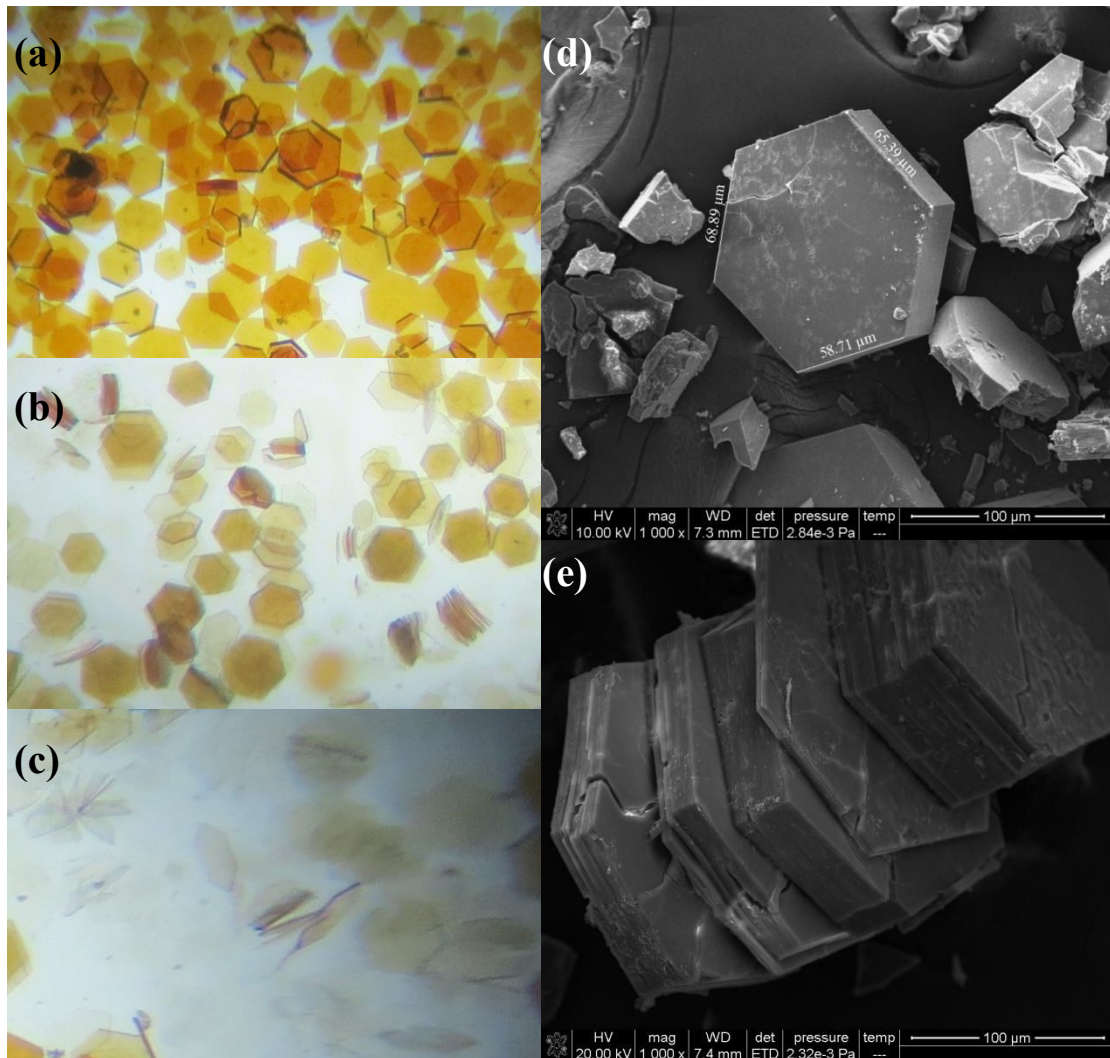


Figure S11. Photographs of the crystals of **2** in air (a); in water for 1 min (b); in water for 24h (c) and the magnified SEM images of **2** in air (d); in water (e). These result showing there are obvious exfoliation phenomenon occurs on the hexagon yellow crystals of **2**. After a certain period of time (24h), it is observed that the exfoliation phenomenon still exist, further confirming the nanosheets of **2** are stable in wet air.

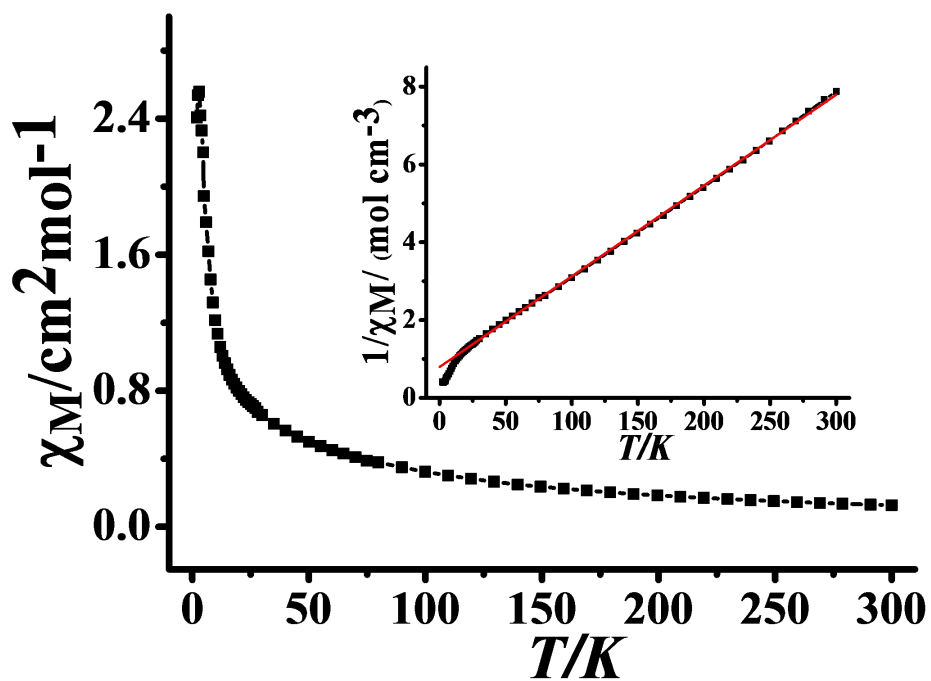


Figure S12. Plots of the χ_M product vs T for **1**; inset: χ_M^{-1} vs T

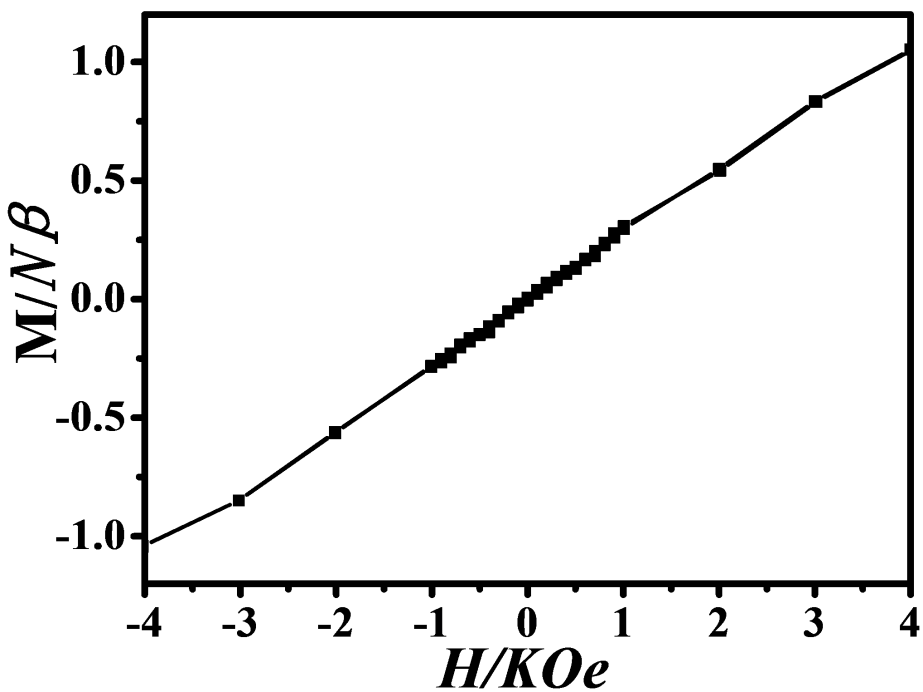


Figure S13. The plot of hysteresis loop at 2K for **1**

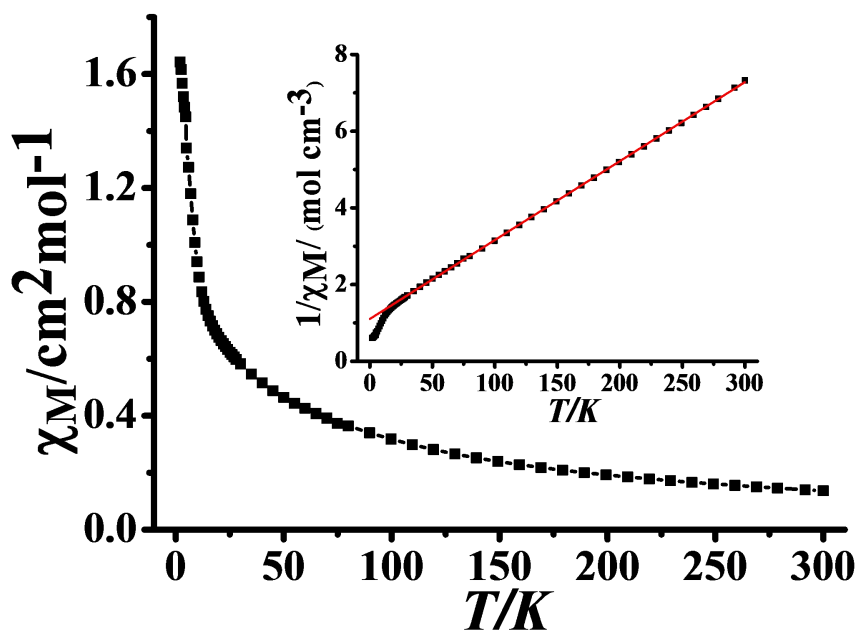


Figure S14. Plots of the χ_M product vs T for **2**; inset: χ_M^{-1} vs T

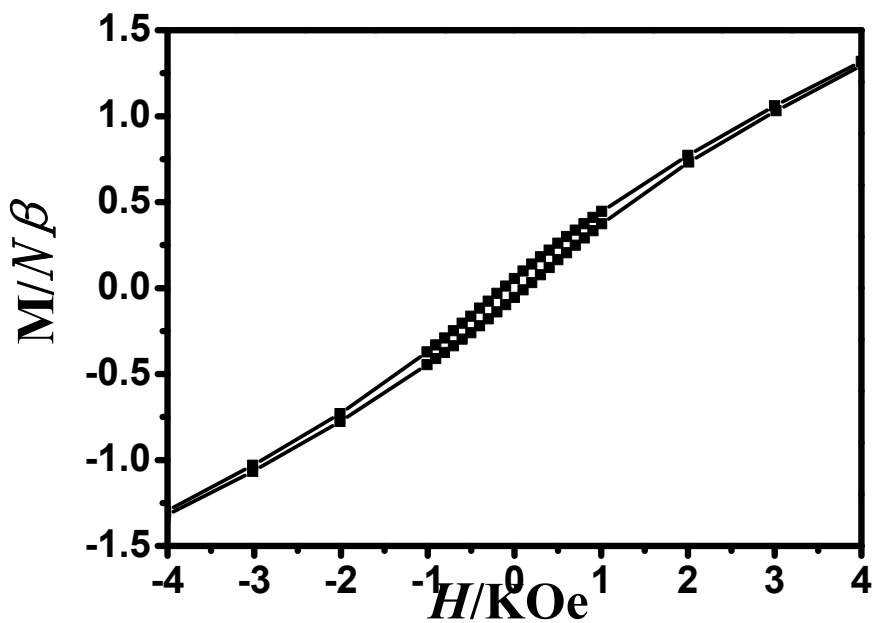


Figure S15. The plot of hysteresis loop at 2K for **2**.

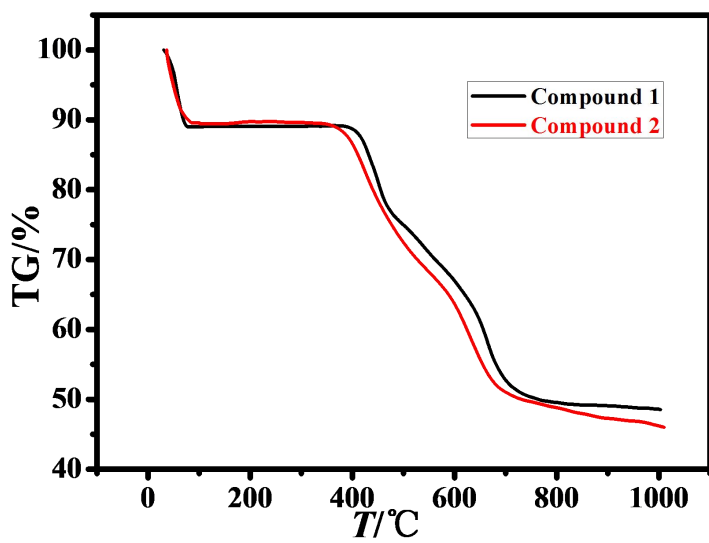


Figure S16. The TG curves of compounds **1–2**.